NANO LETTERS

2009
Vol. 9, No. 12
3996-4000

Charge Carrier Motion in Disordered Conjugated Polymers: A Multiscale Ab Initio Study

Nenad Vukmirović* and Lin-Wang Wang

Computational Research Division, Lawrence Berkeley National Laboratory, Berkeley, California 94720

Received July 6, 2009; Revised Manuscript Received September 15, 2009

ABSTRACT

We developed an ab initio multiscale method for simulation of carrier transport in large disordered systems, based on direct calculation of electronic states and electron−phonon coupling constants. It enabled us to obtain the never seen before rich microscopic details of carrier motion in conjugated polymers, which led us to question several assumptions of phenomenological models, widely used in such systems. The macroscopic mobility of disordered poly(3-hexylthiophene) (P3HT) polymer, extracted from our simulation, is in agreement with experimental results from the literature.

Semiconducting conjugated polymers have been used in many electronic applications from field-effect transistors,[1,2] light-emitting diodes[3,4] to solar cells[5,6] due to relative ease to synthesize and mold them into different shapes. However, one of the major bottlenecks in conjugated polymer applications is the low carrier mobility.[7] There is therefore a great interest to understand the microscopic factors that determine the mobility and have a reliable tool to predict its value. In the last several decades, transport through disordered organic systems, including conjugated polymers, was traditionally analyzed using the phenomenological models,[8−12] which do not consider the nanoscale structure of the material and contain several fitting parameters. One would certainly like to improve upon this simple picture and get an insight into the microscopic processes in the material. Consequently, in several recent works,[13−17] the transport in organic systems was analyzed by combining small molecule ab initio calculations with classical molecular dynamics (MD) and kinetic Monte Carlo.

In this letter, we present an ab initio multiscale approach for the simulation of transport in disordered systems. The method is based on ab initio calculations of the electronic structure and electron−phonon (e-ph) interaction of the thousands atom systems and links the relevant quantities at four length scales to obtain the mobility of the system. It was applied to simulate the mobility in strongly disordered P3HT polymers. The results obtained for the first time provide direct insight into the microscopic nature of carrier flow in these systems and yield the temperature dependence of the mobility in accordance with experimental results from the literature.

* E-mail: NVukmirovic@lbl.gov.

10.1021/nl9021539 CCC: $
Published on Web 11/13/2009

In disordered organic systems, different mechanisms of carrier mobility are possible. For systems where the e-ph interaction and consequently the polaron effect are strong (such as small molecules), Marcus theory provides a good description for charge transfer between polaron states of different molecules.[18] In systems with weaker e-ph coupling, including the ones considered here, the transport can be described as phonon-assisted hopping[18,19] and the transition rates are then usually modeled using the phenomenological expressions of the Miller-Abrahams type.[18,20] Recently, the importance of conformational dynamics in the case of partially ordered organic systems was discussed.[16] In the case of strongly disordered polymers considered here, the conformational motion of polymer chains is much slower than the electron dynamics.[21] Therefore we adopt the approach where the electronic states are static, while the fast nuclear vibrations (phonons) around the conformation cause the transitions between these states, in line with the traditional view in disordered polymers.[8−12] Both intrachain and interchain hopping are therefore treated on equal footing. The polaronic relaxation of carrier states was not included since recent density functional theory calculations[22,23] have shown that polaron binding energy in long straight polythiophene chains is of the order of few millielectronvolts only, suggesting that it is irrelevant for transport. We have performed additional calculations[24] that implied that this conclusion can be largely extended to carrier localized on a part of a long disordered chain, which is the case studied here.

Our recently developed[25,26] charge patching method (CPM) was used to calculate the electronic states for systems with a few thousand atoms. The CPM gives eigenenergies with

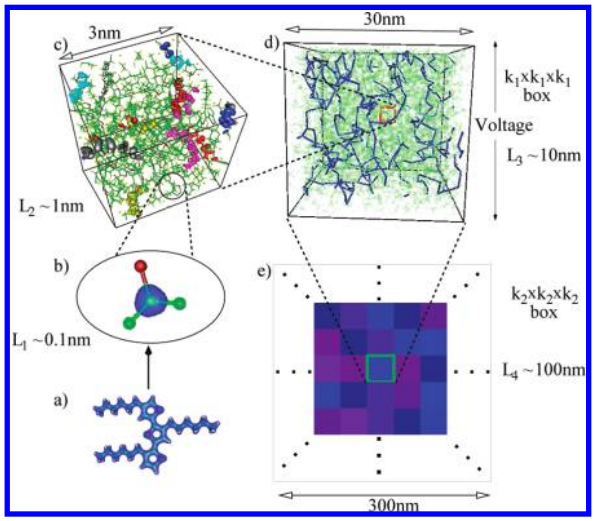

Figure 1. Schematic view of the procedure used for multiscale simulation. (a) The atomic structure of the three unit long oligomer of P3HT and the isosurface of the corresponding charge density. (b) The isosurface of the charge density motif assigned to one of the atoms. (c) Atomic structure and isosurface plot of several valence band wave functions in a 2510 atom P3HT system (length scale L_2). The states from VBM to VBM-6 are shown respectively in dark blue, light blue, red, pink, dark red, yellow, and gray. Isosurfaces in (a), (b), and (c) correspond to 50% probability of finding the charge inside the surface. (d) The spatial distribution of carrier states (green dots) and the current (blue lines) through the structure at the length scale L_3, when the voltage is applied in the direction which is indicated. The currents larger than 5% of the maximal current in the structure are shown. These currents contribute to at least 75% of the current at each cross section perpendicular to the direction in which the voltage is applied. (e) The system at the length scale L_4.

only tens of millielectronvolts error compared with direct ab initio density functional theory (DFT) in local density approximation (LDA) results but with a speed up of thousands of times. More importantly, using the CPM we can efficiently calculate[24] the e-ph coupling constants between electronic states $|i\rangle$ and $|j\rangle$ (which are the eigenstates of the single-particle Hamiltonian) given by $\mathscr{M}_{ij,\alpha} = \langle i|\partial H/\partial v_\alpha| j\rangle$ for all the phonon modes α, where $\partial H/\partial v_\alpha$ is the change of the single-particle Hamiltonian due to the displacement of atoms according to phonon mode α. The CPM calculated $\partial H/\partial v_\alpha$ is within 10% of the directly calculated DFT results.[24] If direct DFT calculations were used, thousands (for each phonon mode) of such self-consistent calculations would be needed to calculate the e-ph coupling constants, each with thousands of atoms, which would make such calculations impossible. Since we are interested in the mobility of holes, the LDA band gap problem does not affect our results. Our calculation is done using norm conserving pseudopotentials with plane wave kinetic energy cutoff of 60 Ry.

Starting from such electronic structure calculations, we developed a multiscale simulation of hole transport in strongly disordered (amorphous) P3HT polymer. The simulation was performed in a manner that bridges four length scales (see Figure 1), the $L_1 \sim 1$ Å scale where the relevant quantity is the contribution of a given atom to the electronic charge density of the system (so-called charge-density motif), the $L_2 \sim 1$ nm scale with the wave functions, the $L_3 \sim 10$ nm scale with carrier states considered as points in space connected by conductors, and the $L_4 \sim 100$ nm scale where the system is considered as the continuum with spatially varying conductivity.

At the length scale L_2, the atomic structure of amorphous P3HT material in the region of space in the shape of a cubic box of the ~3 nm size containing 2510 atoms (this size of the box corresponds to the experimental density of P3HT[24]) is constructed by performing a classical MD simulation using a simulated annealing procedure.[24] The link between the quantities at length scales L_1 (charge density motifs) and L_2 (wave functions and energies) is obtained[24] using the CPM.[25−27] Sixteen top valence band states that cover the ~0.8 eV spectral region relevant for hopping transport have been calculated. Seven top of these states are presented in Figure 1c. The wave functions are localized to a region of space typically containing 3−6 rings of the polymer chain, which is significantly smaller than the box size. Therefore, each of the states exhibits a typical environment as in an infinite material, in terms both of the presence of other states located close to it and in terms of the phonon modes available for coupling. All the phonon modes in a given L_2 system were calculated using classical force field[24] which describes well the vibrational behavior of such organic systems. The e-ph coupling constants $\mathscr{M}_{ij,\alpha}$ for all the relevant electronic states and phonon modes were calculated using the CPM and were subsequently used to calculate the transition rates W_{ij} between hole states as[24]

$$W_{ij} = \pi \sum_\alpha \frac{|\mathscr{M}_{ij,\alpha}|^2}{\omega_\alpha}[(N_\alpha + 1)\delta(\varepsilon_i - \varepsilon_j - \hbar\omega_\alpha) + N_\alpha \delta(\varepsilon_i - \varepsilon_j + \hbar\omega_\alpha)] \quad (1)$$

where N_α is the phonon occupation number at a temperature T, $\hbar\omega_\alpha$ is the phonon energy of mode α, and ε_i is the single particle energy of state i.

To gain sufficient information to make a bridge from L_2 to L_3, the above calculations performed at L_2 were repeated $m_1 = 10$ times with different atomic structures arising from different initial conditions in MD simulations. Furthermore, to get a more accurate description of energy fluctuations of the valence band maximum (VBM) level, additional $m_2 = 100$ calculations were performed for VBM energy (without calculating the e-ph coupling constants or other electronic states). A Gaussian distribution of the VBM level with a standard deviation of 108 meV was obtained.

At the length scale L_3, a box, $k_1 = 10$ times larger than L_2, is constructed from $k_1 \times k_1 \times k_1$ equal small boxes (Figure 1d). Each of these boxes is filled with a randomly chosen and randomly oriented one of the m_1 structures obtained at L_2. All the eigenenergies of the states within a small box are further shifted by the same random number such that the VBMs of small boxes satisfy the calculated 108 meV width Gaussian distribution. At low electric fields and low carrier density, hopping transport is fully equivalent[28] to the transport through the conductor network where the conductance between the sites i and j is $G_{ij} = [e^2/(k_B T)]n_i W_{ij} = [e^2/(k_B T)]n_j W_{ji}$, where n_i is the equilibrium occupation of

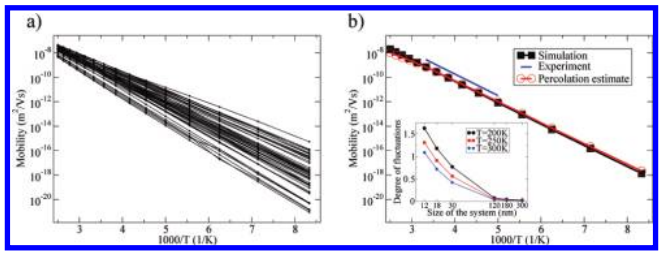

Figure 2. Mobility of the disordered P3HT polymer. (a) Temperature dependence of the mobility in the x, y, and z direction for m_3 different calculations at length scale L_3. (b) Temperature dependence of the mobility of the whole system (squares). Estimate based on percolation (circles). Experimental results[29,30] (line). The inset shows the dependence of the degree of fluctuations in the mobility (defined in the text) on the size of the system.

state i given by the Boltzmann distribution, e is the elementary charge, and k_B is the Boltzmann constant. The transition rates between states from the same small box are available from the calculation on L_2, as discussed above. On the other hand, to calculate the transition rates between the states from neighboring boxes, the e-ph coupling elements are approximated in a manner which retains their statistical averages.[24] The equivalent conductance, and consequently the mobility, in each of the three directions is then calculated. The scattered results presented in Figure 2a for $m_3 = 16$ different random realizations of the L_3 system indicate that at this length scale the fluctuations are still large.

As a final step that bridges L_3 and L_4, a new system is constructed containing $k_2 \times k_2 \times k_2$ boxes (where $k_2 = 10$ was chosen). Each of the boxes of the new system corresponds to one of the randomly chosen and randomly oriented m_3 realizations on the length scale L_3. The conductance of the whole system at L_4 is then calculated by treating these boxes as continuum objects.[24] The mobility in the direction d ($d = x$, y, or z) is then given as $\mu_d = G_d/(neL)$, where G_d is the equivalent conductance in the d direction, n is the concentration of carriers, and L is the size of the box at this length scale (~300 nm). The fluctuations among different realizations of the system and among mobilities in different directions are small and the mobility is therefore a well-defined quantity at this length scale. The obtained mobility μ is presented in Figure 2b. The degree of fluctuations defined as the standard deviation of $\log_{10}\mu$, calculated for different system sizes, is presented in the inset in Figure 2b and indicates that ~100 nm can be identified as the length scale where mobility is well-defined.

A comparison with experimental results[29,30] for the mobility of amorphous P3HT is made in Figure 2b. The fit to the experimental results[30] in the form $\mu = \mu_0 \exp[-E_A/(k_B T)]$ gives an activation energy of $E_A = 350$ meV and the mobility at room temperature of $\mu_{300K} = 2.8 \times 10^{-9}$ m^2/Vs. The simulation gives $E_A = 347$ meV and $\mu_{300K} = 0.71 \times 10^{-9}$ m^2/Vs. An excellent agreement is therefore obtained for the activation energy and a correct order of magnitude for the mobility. We note that our results correspond to a fully disordered polymer. One certainly expects that ordering, which might be present in some degree even in experimentally disordered P3HT polymers, would increase the mobility[31] and decrease the activation energies.[31,32]

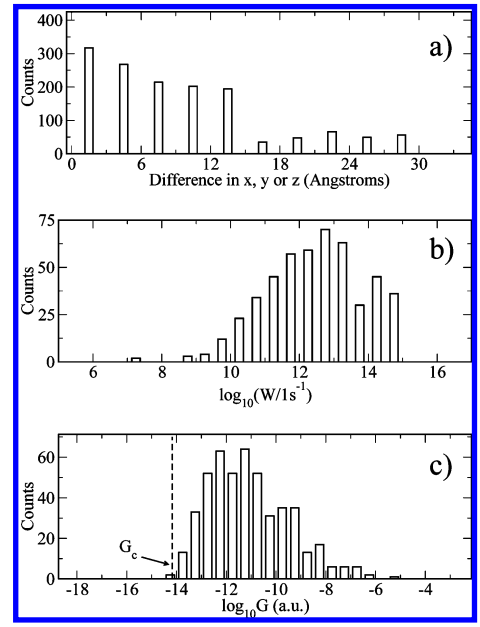

Figure 3. The distribution of hopping distances, transition rates and conductances on the relevant current path at room temperature (a) the hopping distances in x, y, or z direction, (b) the transition rates, and (c) the conductances.

To build a microscopic picture of carrier flow through the material, we return to the simulations at L_3. The current distribution at room temperature for one of the realizations of the system is visualized in Figure 1d, where the most relevant (according to the criterion specified in the caption of Figure 1) current paths are indicated. The distributions of hopping distances and transition rates on these paths shown in Figure 3a,b indicate that hopping over a range of distances is relevant, which supports the picture of the variable range hopping models.[19]

The distribution of current in terms of the energies of the states that carry the current is presented in Figure 4b. The states closest to the top of the valence band, although mostly populated, only weakly contribute to current, due to the low density of states at that energy range for the carriers to jump to nearby states. As a results, most of the current is conducted by carriers ~0.3 eV below the VBM, which leads to the 347 meV activation energy E_A obtained above. The density of states in the region of relevant energies (Figure 4a) does not follow a phenomenological Gaussian distribution, which is usually assumed in the model calculations. (However, the VBM energy of the L_2 boxes does follow a Gaussian distribution, as discussed before.) The justification for using the Gaussian distribution for density of states usually comes from considerations that the states in the polymer originate from VBM states of several polymer units and the fluctuation is due to the variations in the segment length and the local environment. One should note, however, that the VBM-1 state of longer oligomers can have energies in the region of VBM states of the shorter ones[33] (Figure 4c therein). Therefore, a more complicated distribution than the simple Gaussian is formed. We note that the density of states distribution very similar to ours was obtained in a very recent work on ordered P3HT polymer at room temperature.[34]

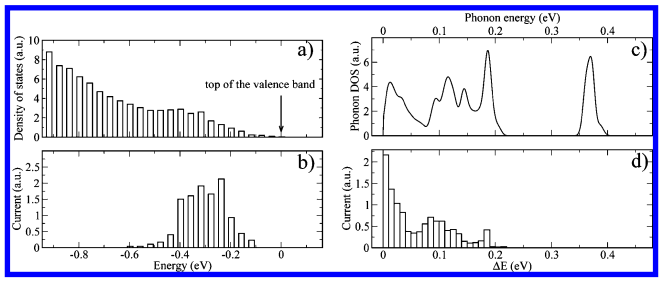

Figure 4. The distribution of current with respect to hole energy and the phonon modes involved. (a) The density of hole states. (b) The distribution of current in energy space. (c) The phonon density of states. (d) The distribution of current due to transitions of different energy. The distributions of current with respect to energy (b,d) were calculated in the following way. An energy equal to the average (in case b) or absolute difference (in case d) of the two states involved in the transition was assigned to each transition. A certain reference plane is chosen then. The contribution of each transition to the current through that plane is determined and a histogram is formed by adding the contributions that fall in each of the energy windows. The final histogram in panels b and d is obtained by averaging over such histograms for several different reference planes.

In several recent works,[35,36] the importance of high frequency phonons for the charge transport in small molecule based organic semiconductors[37] has been discussed. The contributions of different phonon modes to the current in our system are illustrated in Figure 4d. All phonon modes except the high frequency C−H modes at ∼380 meV are involved in the transport, which is in stark contrast to the usual assumption, inherent from Miller−Abrahams form,[8−12,20] of hopping rates that only low frequency acoustic modes are involved. The histogram of phonon mode contribution largely follows the phonon spectrum (Figure 4c) with a difference that it becomes progressively damped as the energy increases.

One simple approach to estimate the mobility of a disordered system is based on percolation theory. A critical conductance G_c is defined for the system from the following criterion: the connections between the sites with the conductance G_{ij} larger than G_c form a percolation network which spans the system. The percolation network can be formed if the number of connections per site is larger than a_c, which is characteristic for a given type of network. The conductivity is then estimated from the relation $\sigma = G_c/L_c$, where L_c is the characteristic length scale for the network. We find that $L_c = 1.5$ nm, which is within the range of hopping distances in Figure 3a and $a_c = 3.2$ can provide an excellent fit (for the temperature dependence) to our directly calculated results, as shown in Figure 2b. The resulting G_c does include all the actively used G_{ij}, as shown in Figure 3c. This and Figure 1d are both in support of the percolation model.

To summarize, we found the following: (1) The macroscopic conductivity is controlled by a small number of microscopic percolation paths that resemble the lightning bolts. (2) The mobility of a polymer block smaller than 100 nm fluctuates depending on the detailed atomic configuration. This sets a practical limit for the devices made of such materials when device uniformity is important. (3) The whole phonon spectrum except for the high frequency C−H modes is responsible for current in contrast to a usual picture that only acoustic phonons are relevant. (4) There are large fluctuations in hopping distances and transition rates along the relevant current paths, which supports the variable range hopping picture. (5) The electronic density of states in the spectral region where carriers are mobile has a distribution that differs from a Gaussian that is usually assumed in the phenomenological transport models. Many of these predictions await for future experimental confirmations.

Most importantly, we have developed a new accurate ab initio approach to study the transport in disordered organic systems. Furthermore, the ability to evaluate the e-ph coupling of large systems opens the way to study many other important problems, from transport to carrier cooling and dynamics in both organic and inorganic nanosystems.

Acknowledgment. This work was supported by the DMS/BES/SC of the U.S. Department of Energy under Contract No. DE-AC02-05CH11231. It used the resources of National Energy Research Scientific Computing Center (NERSC).

Supporting Information Available: The details of the procedure for charge density motif generation, the procedure for generation of the atomic structure, the calculation of wave functions and energies, the calculation of phonon spectrum and electron−phonon coupling, the role of polarons, the role of broadening of the delta function, the convergence check, the procedure for calculating the electron−phonon coupling elements of the states from neighboring boxes and the calculation of equivalent conductances. This material is available free of charge via the Internet at http://pubs.acs.org.

References

(1) Sirringhaus, H.; Brown, P. J.; Friend, R. H.; Nielsen, M. M.; Bechgaard, K.; Langeveld-Voss, B. M. W.; Spiering, A. J. H.; Janssen, R. A. J.; Meijer, E. W.; Herwig, P.; de Leeuw, D. M. *Nature* **1999**, *401*, 685–688.
(2) Kline, R. J.; McGehee, M. D.; Toney, M. F. *Nat. Mater.* **2006**, *5*, 222–228.
(3) Burroughes, J. H.; Bradley, D. D. C.; Brown, A. R.; Marks, R. N.; Mackay, K.; Friend, R. H.; Burns, P. L.; Holmes, A. B. *Nature* **1990**, *347*, 539–541.
(4) Yap, B. K.; Xia, R.; Campoy-Quiles, M.; Stavrinou, P. N.; Bradley, D. D. C. *Nat. Mater.* **2008**, *7*, 376–380.
(5) Sariciftci, N. S.; Braun, D.; Zhang, C.; Srdanov, V. I.; Heeger, A. J.; Stucky, G.; Wudl, F. *Appl. Phys. Lett.* **1993**, *62*, 585–587.
(6) Kim, Y.; Cook, S.; Tuladhar, S. M.; Choulis, S. A.; Nelson, J.; Durrant, J. R.; Bradley, D. D. C.; Giles, M.; McCulloch, I.; Ha, C.-S.; Ree, M. *Nat. Mater.* **2006**, *5*, 197–203.
(7) Tuladhar, S. M.; Sims, M.; Kirkpatrick, J.; Maher, R. C.; Chatten, A. J.; Bradley, D. D. C.; Nelson, J.; Etchegoin, P. G.; Nielsen, C. B.; Massiot, P.; George, W. N.; Steinke, J. H. G. *Phys. Rev. B* **2009**, *79*, 035201.
(8) Baranovskii, S. D.; Cordes, H.; Hensel, F.; Leising, G. *Phys. Rev. B* **2000**, *62*, 7934–7938.
(9) Arkhipov, V. I.; Heremans, P.; Emelianova, E. V.; Adriaenssens, G. J.; Bassler, H. *Appl. Phys. Lett.* **2003**, *82*, 3245–3247.
(10) Borsenberger, P. M.; Pautmeier, L.; Bassler, H. *J. Chem. Phys.* **1991**, *94*, 5447–5454.
(11) Vissenberg, M. C. J. M.; Matters, M. *Phys. Rev. B* **1998**, *57*, 12964–12967.
(12) Pasveer, W. F.; Cottaar, J.; Tanase, C.; Coehoorn, R.; Bobbert, P. A.; Blom, P. W. M.; de Leeuw, D. M.; Michels, M. A. J. *Phys. Rev. Lett.* **2005**, *94*, 206601.
(13) Kirkpatrick, J.; Marcon, V.; Nelson, J.; Kremer, K.; Andrienko, D. *Phys. Rev. Lett.* **2007**, *98*, 227402.
(14) Deng, W.-Q.; Goddard, W. A. *J. Phys. Chem. B* **2004**, *108*, 8614–8621.

(15) Athanasopoulos, S.; Kirkpatrick, J.; Martinez, D.; Frost, J. M.; Foden, C. M.; Walker, A. B.; Nelson, J. *Nano lett.* **2007**, *7*, 1786–1788.
(16) Troisi, A.; Cheung, D. L.; Andrienko, D. *Phys. Rev. Lett.* **2009**, *102*, 116602.
(17) Kwiatkowski, J. J.; Frost, J. M.; Nelson, J. *Nano Lett.* **2009**, *9*, 1085–1090.
(18) Coropceanu, V.; Cornil, J.; da Silva Filho, D. A.; Olivier, Y.; Silbey, R.; Bredas, J.-L. *Chem. Rev.* **2007**, *107*, 926–952.
(19) Coehoorn, R.; Pasveer, W. F.; Bobbert, P. A.; Michels, M. A. J. *Phys. Rev. B* **2005**, *72*, 155206.
(20) Miller, A.; Abrahams, E. *Phys. Rev.* **1960**, *120*, 745–755.
(21) A value of ∼100 ps can be estimated from Figure 3b as the longest time scale for relevant electronic transitions and we have checked that ∼100 ps molecular dynamics simulation does not change the shape of the chains.
(22) Meisel, K. D.; Vocks, H.; Bobbert, P. A. *Phys. Rev. B* **2005**, *71*, 205206.
(23) Zade, S. S.; Bendikov, M. *Chem.—Eur. J.* **2008**, *14*, 6734–6741.
(24) See Supporting Information.
(25) Vukmirović, N.; Wang, L.-W. *J. Chem. Phys.* **2008**, *128*, 121102.
(26) Vukmirović, N.; Wang, L.-W. *J. Phys. Chem. B* **2009**, *113*, 409–415.
(27) Wang, L.-W. *Phys. Rev. Lett.* **2002**, *88*, 256402.
(28) Ambegaokar, V.; Halperin, B. I.; Langer, J. S. *Phys. Rev. B* **1971**, *4*, 2612–2620.
(29) Tanase, C.; Meijer, E. J.; Blom, P. W. M.; de Leeuw, D. M. *Phys. Rev. Lett.* **2003**, *91*, 216601.
(30) Craciun, N. I.; Wildeman, J.; Blom, P. W. M. *Phys. Rev. Lett.* **2008**, *100*, 056601.
(31) Sirringhaus, H.; Tessler, N.; Friend, R. H. *Science* **1998**, *280*, 1741–1744.
(32) Goh, C.; Kline, R. J.; McGehee, M. D.; Kadnikova, E. N.; Frechet, J. M. J. *Appl. Phys. Lett.* **2005**, *86*, 122110.
(33) Hutchison, G. R.; Zhao, Y.-J.; Delley, B.; Freeman, A. J.; Ratner, M. A.; Marks, T. J. *Phys. Rev. B* **2003**, *68*, 035204.
(34) Cheung, D. L.; McMahon, D. P.; Troisi, A. *J. Am. Chem. Soc.* **2009**, *131*, 11179–11186.
(35) Coropceanu, V.; Sanchez-Carrera, R. S.; Paramonov, P.; Day, G. M.; Bredas, J.-L. *J. Phys. Chem. C* **2009**, *113*, 4679–4686.
(36) Wang, L. J.; Peng, Q.; Li, Q. K.; Shuai, Z. *J. Chem. Phys.* **2007**, *127*, 044506.
(37) Hannewald, K.; Stojanovic, V. M.; Schellekens, J. M. T.; Bobbert, P. A.; Kresse, G.; Hafner, J. *Phys. Rev. B* **2004**, *69*, 075211.

NL9021539